HHS Public Access

Author manuscript

Angiogenesis. Author manuscript; available in PMC 2018 May 01.

Published in final edited form as:

Angiogenesis. 2017 November ; 20(4): 505–518. doi:10.1007/s10456-017-9561-x.

CXCL10 suppression of hem- and lymph-angiogenesis in inflamed corneas through MMP13

Nan Gao[1,2], **Xiaowei Liu**[6], **Jiayin Wu**[3], **Juan Li**[4], **Chen Dong**[5], **Xinyi Wu**[3], **Xiao Xiao**[4], and **Fu-Shin X. Yu**[1,2]

[1]Department of Ophthalmology/Kresge Eye Institute, Wayne State University School of Medicine, 4717 St. Antoine Blvd, Detroit, MI 48201, USA

[2]Department of Anatomy/Cell Biology, Wayne State University, Detroit, MI 48201, USA

[3]Department of Ophthalmology, Qilu Hospital of Shandong University, Jinan, Shandong Province, China

[4]Eshelman School of Pharmacy, University of North Carolina at Chapel Hill, Chapel Hill, NC 27599, USA

[5]College of Biological Engineering, Henan University of Technology, Zhengzhou 450051, Henan, China

[6]Department of Ophthalmology, Peking Union Medical College Hospital, Peking Union Medical College, Chinese Academy of Medical Sciences, Beijing, China

Abstract

Though not present in the normal adult cornea, both hem- and lymph-angiogenesis can be induced in this tissue after an inflammatory, infectious, or traumatic insult. We previously showed that the chemokine CXCL10 plays a key role in eradicating invading *Candida* (*C.*) *albicans* in C57BL6 mouse corneas. However, even after the clearance of pathogens, infection-induced inflammation and angiogenesis continue to progress in the cornea. The aim of this study is define the role of CXCL10 as a major angiostatic factor in modulating cornea angiogenesis in B6 mouse corneas under pathogenic conditions. We showed that epithelial expression of CXCL10, driven by AAV9 vector, suppressed both infection- and inflammation-induced hem and lymph angiogenesis, whereas the neutralization of CXCL10 as well as its receptor CXCR3 greatly promoted these processes. The inhibitory effect of CXCL10 was unrelated to its antimicrobial activity, but through the suppression of the expression of many angiogenic factors, including VEGFa and c, and MMP-13 in vivo. Inhibition of MMP13 but not TIMPs, attenuated suture-induced neovascularization but had no effects on CXCL10 expression. Strikingly, topical application of CXCL10 post-*C. albicans* infection effectively blocked both hem- and lymph-angiogenesis and preserved the integrity of sensory nerves in the cornea. Taken together, CXCL10 has strong inhibitory effects on neovascularization, whereas MMP13 is required for neovascularization in *C.*

Correspondence to: Fu-Shin X. Yu.

Electronic supplementary material The online version of this article (doi:10.1007/s10456-017-9561-x) contains supplementary material, which is available to authorized users.

albicans-infected corneas and the local application of CXCL10 or MMP13 inhibitors, alone or as adjuvant therapy, may target hem- and lymph-angiogenesis in the inflamed corneas.

Keywords

Angiogenesis; Candida albicans keratitis; CXCL10; Cornea

Introduction

Corneal avascularity is a prerequisite for the maintenance of vision. The cornea is the forefront tissue in the visual pathway, providing a clear structure for the passage of light. It is also one of few tissues in the body that is normally devoid of any vascular blood or lymphatic structures. Studies have identified multiple mechanisms, including the expression of anti-angiogenic factors, lack of pro-angiogenic factors, and expression of soluble VEGF receptors as underlying mechanisms for maintaining cornea avascularity [1–5]. However, many pathological conditions such as trauma, chemical injury, inflammation, and infection can break the balance of pro- and anti- angiogenic actions, resulting in hem-angiogenesis (HG; the development of new blood vessels) and lymph-angiogenesis (LG; the development of new lymphatic vessels) [6–9]. While presence of blood vessels certainly obstructs the light pass, the formation of new vascular structures in areas that were previously avascular will induce aberrations in the unique organized structure of the cornea, resulting in a decrease in visual acuity or even blindness [10, 11]. As for lymph-angiogenesis, in addition for obstruction of corneal stroma structure, lymphatic vessels may contribute to a decreased success rate of corneal transplantation in a vascularized cornea by accelerating antigen recognition, resulting in graft rejection [7, 12–15]. Hence, Given the simple structure of the cornea, which lacks appendages (e.g., glands) and pre-existing blood- and lymph-vessels, the accessibility of the tissue, and the availability of a battery of clinical tests that can be adapted in animal models, the cornea has been used as an ideal in vivo model for HG research over 50 years [16], and more recently for LG [17].

Fungal keratitis, such as that caused by *C. albicans* can result in devastating ocular damage, including neovascularization [17], if not diagnosed and treated promptly [18]. We adopted a B6 mouse *C. albicans* model in which the invading pathogens were eliminated spontaneously within 3 days of infection while inflammation lingered on for about two weeks. In *C. albicans*-infected B6 mouse corneas, we also noticed visible neovascularization at day 3, which peaked at day 7, and retraction thereafter, similar to reports by others. [17, 19] By day 14, the corneas were mostly disease free. Since at and/or after 3 dpi there was no recoverable *C. albicans* from the infected corneas, the formation of new vessels towards the center of the cornea is likely the result of lingering host inflammatory response. The underlying mechanisms controlling inflammation, inflammation associated angiogenesis, and their resolution remain incompletely understood.

CXCL10 is a pleiotropic molecule capable of exerting potent biological functions, including promoting the chemotactic activity of $CXCR3^+$ cells, inducing apoptosis, regulating cell growth and proliferation as well as angiogenesis in infectious and inflammatory diseases and

cancer [20–24]. CXCL10 is a member of the interferon-inducible tripeptide motif Glu-Leu-Arg-negative (ELR^-) CXC chemokines [25]. This chemokine, along with CXCL9 and CXCL11, signals through a G-protein-coupled receptor, CXCR3 which is expressed primarily on activated T lymphocytes and NK cells, and functions in the recruitment of these cells to the sites of infection and inflammation [26–29]. In addition to their roles in leukocyte recruitment, CXCR3 ligands exert direct antimicrobial effects that are comparable to the effects mediated by cationic antimicrobial peptides, including defensins [30]. In previous studies, we showed that CXCL10 participated in corneal innate defense against microbial infection, including as an epithelial-expressed antimicrobial peptide and chemokine to attract cells such as Natural killer cells [31]. Our studies revealed a complicated signaling pathway, including TLR-dependent epithelial expression of CXCL10, CXCR3-dependent-NK cell infiltration and production of IFN-γ, the activation of IRF1, that further augmented expression of CXCL10 in both infiltrated and residential cells [31, 32]. We proposed that the induced and persistently expressed CXCL10 in inflammatory corneas may serve as an endogenous factor that prevents angiogenesis and control vessel regression.

In this study, we used two corneal neovascularization models and assessed not only hem- but also lymph-angiogenesis in the avascular corneas. We showed strong inhibitory effects of CXCL10 on corneal hem- and lymph-angiogenesis and identified MMP-13 as a downstream effector that required for the growth of the vessels into the cornea. Our data also showed potential of gene therapy to treated corneal infection and neovascularization and topical application of CXCL10 as an adjunctive reagent to accelerate fungal clearance, inflammation resolution, and/or to reduce or prevent neovascularization in the cornea.

Methods

Fungi

CA strain SC5314, a clinical isolate capable of producing experimental keratomycosis, was cultured on YPD agar (Sigma) for 3 days at 25 °C. Colonies were harvested after 3 days of inoculation and diluted in sterile phosphate-buffered saline (PBS) to yield 2×10^5 colony-forming units (CFU)/μL based on the optical density (OD) at 600 nm, using a predetermined OD_{600} conversion factor of 1 OD = 3×10^7 CFU/ml.

Animals

Wild-type C57BL6 (B6) mice (8 weeks of age; 20–24 g weight) were used. Animals were treated in compliance with the ARVO Statement on the Use of Animals in Ophthalmic and Vision Research. The Institutional Animal Care and Use Committee of Wayne State University approved all animal procedures.

AAV-9 mediated overexpression of CXCL10 in B6 mouse corneas

AAV-2-9 were first tested for their effectiveness in the expression of GFP in the cornea and AAV-9 was found most effective and therefore was used. Mice were subconjunctivally injected with 5 μl AAV9-GFP or -CXCL10 (3×10^{12}/ml). The expression of CXCL10 in corneas was monitored by immunostaining 14 days after injection.

Infection procedure

Mice were anesthetized with ketamine/xylazine and placed beneath a stereoscopic microscope at a magnification of 40 ×, and the cornea of the left eye of each mouse was wounded with three 1-mm incisions using a sterile 25-gauge needle. A 5 μl suspension containing 10^5 CFU of *C. albicans* strain SC5314 was applied to the surface of the scarified cornea. Eyes were examined daily to monitor the disease progression. For determining if CXCL10 prevents hem- and hymph-angiogenesis in infected corneas, B6 mouse corneas were inoculated with 1.0×10^5 CFU of *C.* albicans. Topical solution containing lubricant were used to dissolve CXCL10 (25 μg/ml) and then applied starting 6 or 16 hpi and after then every 3 h. The corneas were photographed daily.

To define the role of MMP13 and Timp1 in corneal angiogenesis, 5 μl MMP13 inhibitor (10 ng/μl) (EMD Millipore, MA), Timp1 SiRNA (20 μM, Dharmacon) or Non-Targeting SiRNA (20 μM, Dharmacon) SiRNA was subconjunctivally injected prior 24 h to suture and reinjected every two days. For suture-induced corneal hem-and lymph-angiogenesis, three 11-0 nylon sutures (Serag Wiessner, Naila, Germany) were placed intrastromally into the right cornea. Each group comprised 5 mice. Eyes were taken photos with slit-lamp daily to monitor the disease progression.

Fungal burden in the cornea

Corneas ($n = 5$/group) from *C. albicans*-infected mice were collected, and the number of viable bacteria was determined by the plate count method. Individual corneas were homogenized in sterile PBS, and aliquots (100 μl) of serial dilutions were plated onto YPD agar plates in triplicates. The plates were incubated overnight at 37 °C and bacterial colonies were counted. The results were expressed as the mean number of CFU/cornea ± standard error of the mean.

Suture-induced corneal hemangiogenesis and lymphangiogenesis

Mice were subconjuctivally injected with 5 μl AAV9-GFP or -CXCL10 (3×10^{12}/ml). The expression of CXCL10 in corneas was monitored by immunostaining 14 days after injection. To define the role of MMP13 and Timp1 in corneal angiogenesis, 5 μl MMP13 inhibitor (10 ng/μl) (EMD Millipore, MA), Timp1 SiRNA (20 μM, Dharma-con) or Non-Targeting SiRNA (20 μM, Dharmacon) SiRNA were subconjuactivally injected prior 24 h to suture and reinjected every two days. For suture-induced corneal hemangiogenesis and lymphangiogenesis, three 11-0 nylon sutures (SeragWiessner, Naila, Germany) were placed intrastromally into the right cornea. Each group comprised 5 mice. Daily photos of the eyes were taken with a slit lamp to monitor disease progression.

RT-PCR and real-time PCR

Mouse cornea RNA was extracted using RNeasy Mini Kit (QIAGEN), according to the manufacturer's instructions. cDNA was generated with an oligo (dT) primer (Invitrogen) followed by analysis using real-time PCR with the Power SYBR Green PCR Master Mix (AB Applied Biosystems, University Park, IL) based on the expression of β-actin. Generated cDNA was amplified by PCR by using primers for mouse Cxcl10, Cxcr3 and β-actin. The PCR products and the internal control β-actin were subjected to electrophoresis on 1%

agarose gels containing ethidium bromide. Stained gels were captured by using a digital camera. The following primer pairs were used: 5′-GACGGCCAGGTCATCAC-TATTG-3′, 5′-AGGAAGGCTGGAAAAGAGCC-3′ for β-actin, 5′-GGGAAGAAGTTCCACCATCA-3′, 5′-ATGTG GCCTTTTCCAATACG-3′ for VEGFC, 5′-GCAGCTCAT CAAGTGGTTCA-3′, 5′-GGCATTGAAAAACTCCCGT A-3′ for PROX-1, 5′-GCTGCCATTTCTAATAAAGA-3′, 5′-GCACTTCCTTTCACAAA-3′ for Mmp3 and 5′-TG ATGAAACGACAAGC-3′, 5′-CTGGACCATAAAGAAA CTGAA-3′ for Mmmp13, 5′-TCCTTTCTTAGAGGCC AGCA-3′, 5′-ACGTCATACTCGAGCCCATC-3′ for Ser-pine1and 5′-CATGGAAAGCCTCTGTGGAT-3′, 5′-CTC AGAGTACGCCGAGGAAC-3′ for Timp1.

Analyzing the expression profile of angiogenesis-related proteins

Mouse corneas (n = 4/group) were collected, homogenized in PBS with protease inhibitors and 1% Triton X-100. The protein concentration in cell lysates was determined with the bicinchoninic acid detection assay (MicroBCA; Pierce). Proteins were then probed with mouse angiogenesis antibody proteome profiler array R&D system, Minneapolis, MN) according to manufacturer's instructions. In short, in this method proteins are captured by antibodies spotted on a nitrocellulose membrane. Levels of angiogenic factors are then assessed using an HRP-conjugated antibody followed by chemiluminescence detection. Pixel densities were analyzed by Photoshop.

Western blot analyses

Mouse corneas were lysed with radioimmunoprecipitation assay (RIPA) buffer (150 mm NaCl, 100 mm Tris–HCl [pH 7.5], 1% deoxycholate, 0.1% sodium dodecyl sulfate (SDS), 1% Triton X-100, 50 mm NaF, 100 mm sodium pyrophosphate, and 3.5 mm sodium orthovanadate). A protease inhibitor cocktail (aprotinin, pepstatin A, leupeptin, and antipain, 1 mg/mL each) and 0.1 M phenylmethylsul-fonyl fluoride were added to the RIPA buffer (1:1000 dilution) before use. The protein concentration in cell lysates was determined with the bicinchoninic acid detection assay (MicroBCA; Pierce). Proteins were separated by sodium dodecyl sulfate–polyacrylamide gel electrophoresis (SDS-PAGE) in Tris/glycine/SDS buffer (25 mM Tris, 250 mM glycine, and 0.1% SDS) and electroblotted onto nitrocellu-lose membranes (0.45-μm pores; Bio-Rad, Hercules, CA). After blocking for 1 h in Tris-buffered saline/Tween (TBST; 20 mM Tris–HCl, 150 mM NaCl, and 0.5% Tween) containing 5% nonfat milk, the blots were probed with mouse anti-VEGFa (Abcam,1:1000) and β-actin (Sigma1:10,000) antibodies at 4 °C. The membranes were washed with 0.05% (vol/vol) Tween 20 in TBS (pH 7.6) and incubated with a 1:2000 dilution of horseradish peroxidase-conjugated secondary antibodies (Bio-Rad) for 60 min at room temperature. Protein bands were visualized by chemiluminescence (Supersignal reagents; Pierce).

Immunostaining of whole mount corneal tissue

Mice were euthanized, and the entire cornea plus the limbus was excised under the operating microscope. Excised corneas were fixed in 4% paraformaldehyde and stored at 4 °C until further processing. Before staining, radial incisions were made to produce six pie-shaped wedges. Corneas were washed in PBS, incubated in 20 mmol/L prewarmed EDTA for 30 min at 37 °C, and incubated with a 0.2% solution of Triton X-100 in PBS plus 1% bovine

serum albumin (BSA) for 1 h at room temperature. After blocking, the corneas were incubated overnight at 4 °C with 100 μl of mouse CD31 (BD Pharmingen, San Diego, CA), LYVE-1 (AngioBio) or β-tublin-III (Covance) antibody diluted in PBS with 1% BSA. The tissues were then washed five times in PBS. Corneas were then incubated with 100 μl Cy3-conjugated and FITC-conjugated antibody diluted in PBS with 1% BSA for 1 h at room temperature. This was followed by five washes in PBS. Stained tissue whole mounts were placed in Vectashield mounting medium (Vector Lab, Burlingame, CA) onto glass slides and coverslipped. Corneal whole mounts were examined using confocal microscopy (TCSSP2; Leica, Wetzlar, Germany). Negative controls include isotype matched IgG to replace first antibodies, only dilution of the control antibody showing negative staining was used.

Apoptosis and necrosis assay

To detect apoptotic and necrosis cells, human brain hTERT stained with an Annexin V & Apo 2.7-PE kit (BD Biosciences) and mounted with Vectorshield mounting DAPI medium for nuclear staining and examined under an Olympus BX5OF fluorescence microscope (Olympus, Tokyo, Japan) with an ApoTome digital camera.

In vitro assay of the anti-hem- or lymph-angiogenesis of recombinant CXCL10 and conditioned cultured media of human corneal epithelial cells

Human CECs were starved overnight and transfected with 1.5×10^{11} cfu (Recombinant adeno-associated virus vector-2) with inserted DNA that encoded the human CXCL10 with green fluorescence protein as the control. At day 3 post AAV2 infection, fresh medium were replaced and cells were further cultured for 1 day and media collected as conditioned media for the culture of human brain hTERT (hBRVECs) or primary lymphatic endothelial cells (LECs) in Matrigel. Conditioned media of CECs were also used on culture endothelial cells which were subjected to Annexin V and propidium iodide staining for apoptotic and necrotic cells and photographed using Nikon ECLIPSE 90i microscopy.

CXCL10 and CXCR3 neutralization

Mice (n = 5/group/treatment) were anesthetized as prescribed and rabbit anti-murine CXCL-10(2.5 μg/5 μl, Peprotech) or Rabbit anti-Murine CXCR3 (2.5 μg/5 μl, Abnova), and injected subconjunctivally 6 h before *CA* infection.

Statistical analysis

Data were presented as mean ± SD. Statistical differences among three or more groups were identified using one-way ANOVA. Differences were considered statistically significant at $p < 0.05$. Between two groups, an unpaired, two-tailed Student's t test was used to determine statistical significance for data from fungal counts, cytokine ELISA, the MPO assay and clinical scores. Experiments were repeated at least twice to ensure reproducibility.

Results

AAV9 mediated-expression of mCXCL10 in mouse corneal epithelial cells

To assess the role of CXCL10, we first tested the feasibility of expressing the chemokine in the cornea using AAV-mediated gene delivery. Our preliminary data revealed that among several adeno-associated viruses tested, AAV9-GFP resulted in the highest expression of GFP in B6 mouse corneas. Hence, we generated an AAV9 carrying a synthetic gene encoding mouse CXCL10 with AAV9-GFP as a negative control. The AAV-viruses were injected into subconjunctival space. Immunohistochemistry using CXCL10 antibody revealed the expression of CXCL10 in AAV9-CXCL10, but not -GFP, transfected mouse corneas 14 days post-AAV injection (Fig. 1a). The AAV9-mediated CXCL10 expression remained at detectable levels 1 month post-AAV injection; no ocular surface abnormalities were observed in CXCL10 transfected corneas (data not shown). RT-PCR also showed CXCL10 overex-pression in AAV9-CXCL10 injected corneas (Fig. 1a).

CXCL10 through CXCR3 prevents C. albicans-induced hem- and lymph-angiogenesis in the B6 mouse corneas

To assess the effects of CXCL10 on fungal keratitis and on *C. albicans*-induced hem- and lymph-angiogenesis, we either overexpressed CXCL10 through AAV9-mediated transfection or neutralized the endogenously generated molecules using CXCL10 antibody. The progress of keratitis under different experimental conditions was shown with micrographs of the cornea (Fig. 1b). The *CA* keratitis in C57BL/6 mice, or the controls treated with AAV9-GFP or isotope matched IgGs, was moderate at 1 dpi and exhibited mild eye diseases at 7 dpi. AAV-9 mediated CXCL10 expression prevented *C. albicans*-keratitis from occurring while its neutralization increased the severity of keratitis compared to the controls. The presence and progression of vessels in the corneas were assessed using whole mount confocal microscopy (Fig. 1c). In normal eyes, blood and lymph-vessels, detected with antibodies against CD31, the marker for blood vessel endothelial cells, and Lyve-1, the marker for lymphatic endothelial cells, respectively, were only seen in the limbal region, with one major lymph-vessel running in parallel to the limbus-cornea junction and a network of hem-vessels with no free endings pointing to the cornea. In *C. albicans*-infected corneas, a thick vessel(s) was formed along with a parallel lymph-vessel, and numerous new vessels grew into the corneas with free endings. In these corneas, lymphatic vessels were derived from the limbal lymphatic vessel; these corneal vessels branched to form smaller growing vessels. Interestingly, the lymphatic vessels penetrated the cornea much deeper than the hem-vessels. While a similar pattern of neovascularization can be seen in AAV9-GFP transfected corneas, there was no new vessel formation in AAV9-CXCL10-transfected corneas. On the other hand, the neutralization of CXCL10 resulted in robust neovascularization in both number and length of corneal blood (Fig. 1d) and lymphatic vessels (Fig. 1e). Thus, while the over-expression of CXCL10 prevents neovascularization, the endogenously expressed CXCL10 serves as an important anti-angiogenic factor in the cornea in response to *CA* infection.

The only known receptor of CXCL10 is CXCR3. To determine whether the over-expressed CXCL10 acts through CXCR3, we blockaded the CXCL10-CXCR3-signaling pathway

using CXCR neutralizing antibody. As shown in sFig. 1, about 10^3 cfu *C. albicans* were detected in the control corneas while neutralized of CXCL10 or/and CXCR3 resulted in an increase in fungal load of ~1.5 fold. Corneas with CXCL10 overexpression had few recoverable *CA*, a marked decrease in the number of pathogens that remained in the cornea. The protective effect of AAV9-mediated CXCL10 expression was abolished in CXCR3-neutralized corneas (Fig. 2a). Targeting CXCR3 signaling, regardless the expression of CXCL10, resulted in more robust neo-vessel formation in the corneas compared to control antibody-treated corneas (Fig. 2b). Neutralizing CXCR3 significantly increased the blood (Fig. 2c) and lymph (Fig. 2d) vessel length in the control but more dramatic in CXCL10 expressing corneas. Hence, the data indicated CXCL10 acts as a chemokine that binds to CXCR3 to modulate neovascularization in the cornea. The observed effects of epithelial expressed CXCL10 on corneal neovascularization may be related to its ability to induce the collapse of endothelium network (vessel line, sFig. 2A) and necrosis of endothelial cells in vitro (sFig. 2B).

The expression of angiogenic factors is related to the levels of CXCL10 in the C. albicans-infected corneas

Angiogenesis requires coordinated action of a group of genes, which can be functionally characterized as pro- or anti-angiogenic factors. We used a membrane-based antibody array for the parallel determination of the relative levels of selected angiogenesis-related proteins (54 proteins for mouse, R&D system) (sFig. 3). Among 54 antibodies on the membranes of Proteome Profiler™ (ARY015), 14 proteins were detected with different degrees of altered expression in *C. albicans*-infected corneas with or without AAV9-CXCL10 transfection: IGFBP3, MMP3, Osteopontin, Platlet factor 4, Serpine1, thrombospondin2, IL-1α, IL-10, MCP-1, MMP-9, PD-ECGF, pentraxin-3, and VEGFa (sFig. 3A). The relative expression of these 14 genes, including VEGFa, were analyzed according to the Manufacturer's Assay manual, as shown in sFig. 3B. To further assess if VEGF was induced, we performed Western blotting of the whole corneal extracts and detected VEGFa at the protein level in infected (lane G) but not naïve (lane N) and infected and CXCL10 expressing (lane 10) corneas whereas neutralizing CXCL10 (lane α) resulted in a great increase of VEGFa in *C. albicans*-infected corneas (Fig. 3a). There was no VEGFc, which is known to induce lymphangiogenesis [33, 34], on the Proteome Profiler membrane and Western blotting was also unable to detected VEGFc in the same cell extracts in which relatively abundant VEGFa levels were detected (data not shown). We then used RT-PCR to detect VEGFc as well as prospero homeobox 1 (Prox-1), which is a marker of lymphatic endothelial cells [35, 36]. Indeed, both VEGF-c and Prox1 were detected in *C. albicans*-infected and more apparent in the infected corneas with CXCL10 neutralizing antibodies at both 4 and 7 dpi (Fig. 4b). Hence, the anti-angiogenic effect of CXCL10 was at least partially through controlling the expression of VEGFa and VEGFc.

It was of interest to note that when CXCL10 was neutralized and neovascularization was robust, the expression of CXCL4 (*platelet factor* 4, column 4, sFig. 3), an angiostatic chemokine known to bind to CXCR3, was also greatly up-regulated, suggesting that the anti-angiogenic effects of CXCL10 in the cornea may not be replaced by CXCL4.

The expression patterns of MMP3, MMP13, TIMP1 and Serpine1 detected by Proteome Profiler were confirmed using real-time PCR (Fig. 3c). Among these proteinases and proteinase inhibitor, MMP13, was the most highly up-regulated gene in the infected, CXCL10 neutralized corneas.

CXCL10 overexpression prevents suture-induced hem- and lymph-angiogenesis

The fact that there was a great decrease in fungal burden in the corneas transfected with AAV9-CXCL10 suggested that the observed inhibitory effects of overexpressed CXCL10 might be the indirect results of pathogen clearance. To address this issue, we used an inflammation-caused hem- and lymph-angiogenesis model, the standardized suture placement model [37] (Fig. 4). Three sutures were placed in the control, AAV9-GFP, or CXCL10-transfected B6 mouse corneas. The sutures caused corneal lesions and opacification in the corneas, with or without CXCL10 overexpression (Arrowheads, Fig. 4a). Robust neovascularization of both hem- and lymph-vessels towards the sites of suture placements was observed in the control and AAV9-GFP, but not CXCL10 transfected corneas (7d, Fig. 4a, b). In comparing *C. albicans*- and suture-induced neovascularization, we observed that in infected corneas, lymph-vessels were formed in front of hem-vessels (Fig. 1c), whereas in the sutured corneas, hem vessels were formed with great intensity and reached the sites of the sutures, while lymph-vessels were a noticeable distance away (Fig. 4b). In CXCL10-expressing corneas, no vessels grew into the corneas, despite clearly visible inflammation (opacification) around the sutures (Fig. 4). Interestingly, individual CD31-positive cells could be seen in between the limbus and the suture in a nonrandom fashion; they appeared to form lines (AVA-CXCL10, Fig. 4b), suggesting that CXCL10 may not affect vessel endothelial cell migration along a track, but prevent tube formation or induce the dissociation of formed vessels. There were also weakly stained Lyve-1-positive cells. Using cultured human corneal epithelial cells expressing CXCL10, we demonstrated that hTERT immortalized brain endothelial cells [38] and primarily lymph-endothelial cells cultured in the conditioned media derived from AAV2-CXCl10 transfected cells had more Annexin V and pro-pidium iodide positive cells and formed some tube like structures with deteriorating networks (sFig. 2A), suggesting CXCL10, potentially with other epithelial secreted factors, stimulated vesicular endothelial cell necrosis.

MMP13, but not TIMP1, is required for corneal angiogenesis induced by suture

To define the role of MMP13 in corneal angiogenesis, we treated the sutured corneas with either MMP13 specific inhibitor or siRNA targeting TIMP1 (Fig. 5a). Western blotting of TIMP1 of naïve corneas and the corneas treated either with control or TIMP1 siRNA revealed suture-induced expression was downregulated by TIMP1 specific siRNA (Fig. 5b). Targeting TIMP1 expression had minimal effects on neovascularization (Fig. 5a–c). On the other hand, MMP13 inhibitor blocked the formation of the vessels in the sutured corneas, indicating an essential role of MMP13 in neovascularization and suggesting a novel effective target for blocking pathogenic angiogenesis (Fig. 5a–d).

To assess if MMP13 inhibition affects CXCL10 expression, we performed immunohistochemistry analysis (Fig. 6). We previously showed that the naïve cornea did not express CXCL10 [31, 32]. In sutured, control cornea, CXCL10 was expressed primarily in

the epithelial cells (E) while CD31-stained vessels were located in the stroma (arrows); hem-endothelial cells were negative for CXCL10 staining (Fig. 6a). MMP13 inhibitor-treated corneas, on the other hand, lacked detectable vessels, and yet the expression of CXCL10 in epithelial cells (E) was not affected by MMP13 inhibition (Fig. 6b).

Topical CXCL10 inhibits C. albicans induced angiogenesis and preserves the integrity of sensory nerves in B6 mouse corneas

The ideal way to deliver therapeutic reagents to the eye is topical application in the form of eye drops. To that end, we reconstituted 25 μg/ml CXCL10 solution with Thera Tears (Akorn Pharmaceuticals), an over-the-counter eye lubricant, for its ability to increase ocular surface retention (Fig. 7). We assessed the effects of topical application of CXCL10on neovascularization caused as well as innervation by *C. albicans* infection, topical CXCL10 was applied at 16 hpi (Fig. 7). Eye-drops containing CXCL10 improved keratitis but central cornea inflammation remained at 3 dpi, but greatly decreased the opacity of the corneas at 5 and 7 dpi (Fig. 7a). Whole mount staining of CD31 and LYVE-1 revealed that infection induced hem-and lymph-angiogenesis was inhibited by topical CXCL10 (Fig. 7b). Analyses of blood (C) and lymph (Fig. 7d) vessels indicated that topical application of CXCL10 was sufficient to prevent neo-vessel formation in *C. albicans*-infected corneas.

We also assessed sensory nerve fibers and endings in *C. albicans* infected corneas to determine whether fungal infection adversely affects corneal innervation. As shown in Fig. 7e, robust innervation in the form of small c-fibers and the sub-basal nerve plexus was seen in normal untreated corneas with blood vessels only in the limbal region (L) (NL, Fig. 7e). *C. albicans* infection caused new vessel formation in the otherwise avascular cornea and resulted in disappearance of sub-basal nerve endings without significantly affecting nerve fibers (Lubricant, Fig. 7e). Topical CXCL10 prevented blood vessel formation and partially preserved the sub-basal nerve plexus, as evidenced by a higher density of nerve endings compared to that of the control lubricant-treated corneas (Lub + CXCL10, Fig. 7e).

Discussion

In this study, we showed that epithelial-expressed CXCL10 acts as an intrinsic inhibitor to mediate both hem- and lymph-angiogenesis in the infected and inflammatory corneas and manipulation of CXCL10 expression can control angiogenesis in vivo. We first documented AAV-mediated CXCL10 expression in corneal epithelial cells and demonstrated that overexpression of CXCL10 prevents new vessel formation under the conditions that favor angiogenesis. Our data showed that CXCL10 functions as an anti-angiogenic factor through its receptor CXCR3 expressed in infiltrated cells and vascular endothelial cells directly and through controlling the expression of other angiogenic factors such as VEGFa and c, as well as effectors such as MMP13 and Serpine1 indirectly. Our study also revealed subconjunctival injection and AAV-gene delivery can be used as an effective gene therapy to treat corneal diseases and potentially other ocular diseases, and is the first to show that epithelially-expressed CXCL10 also inhibits lymph-angiogenesis in the cornea, and inhibiting MMP-13 is effective in preventing formation of new vessels. In conclusion, our results suggest that targeted expression of CXCL10 may render tissues or even tumors an

ability to resist abnormal angiogenesis, and raise the possibility of using topical CXCL10 to reduce the rate of rejection in corneal-limbal grafts, through inhibition of lymph-vessel formation, especially for high-risk fungal keratitis patients [39].

Subconjunctival injection is a routinely used ophthalmic procedure, known to be effective in treating corneal diseases and glaucoma without daily multiple applications of eye drops [40, 41]. This route has been used successfully to introduce anti-angiogenic factors to treat angiogenesis, mostly in alkali burn models [42–44]. Similar to an earlier report, we demonstrated that the rAAV was capable of directly delivering CXCL10 to the corneal epithelium by way of subconjunctival injection and was able to deliver sustained, high level expression of the gene in vivo to block *C. albicans* infection and to inhibit angiogenesis while exhibiting limited effects on inflammation. Hence, AAV and subconjunctival injection represent an effective way for gene therapy to treat ocular surface diseases and potentially other ocular diseases such as delivering IL-10 to treat uveitis and CNTF to protect retinal ganglion cells to treat glaucoma [45].

The role of CXCL10 in inhibiting angiogenesis (angiostasis) has been extensively studied in various tissues, including in the cornea [46, 47]. The cornea is unique in that it is avascular. Many factors were identified as intrinsic factors for maintaining the avascularity of the cornea which is adjacent to a highly vascularized tissue, the limbus. However, angiogenesis does occur in injured, infected and/or inflamed corneas, resulting in the loss of vision. As such, a strong inducible anti-angiogenic network in the cornea is expected. The factors and effectors that encounter pro-angiogenic forces under these pathological conditions in the corneas are less well defined. Our previous studies revealed that CXCL10 was one of most highly inducible genes in corneal epithelia cells. The fact that exogenously applied CXCL10, either through forced expression in epithelia or topical application prevents angiogenesis indicates that CXCL10 is a potent angiostatic factor in the stimulated corneas. The demonstrated ability of CXCL10 to prevent corneal angiogenesis in two different models, consisting of both infection and sterile triggers, suggests that CXCL10 is a major anti-angiogenic factor produced by corneal epithelial cells in response to angiogenic stimulation in the cornea. The observation that neutralizing induced CXCL10 or blocking its signaling greatly exacerbates both hem- and lymph-angiogenesis in *C. albican* induced angiogenesis further confirmed the role of CXCL10 in inhibiting new vessel formation. Taken together, we propose that, like expression of FasL and soluble VEGF receptor-1 (sFlt-1) to maintain corneal avascularity in homeostatic corneas, highly inducible, multi-functional CXCL10 is a critical element for counterbalancing the actions of pro-angiogenic factors generated in infected or inflamed corneas.

How might CXCL10 inhibit angiogenesis in the cornea? Our previous studies revealed that while epithelial cells are the major source of CXCL10 in the challenged corneas, they do not express CXCR3. Hence, this epithelial-expressed chemokine is intended for other type(s) of cells in the cornea. Indeed, we showed that when the epithelium is challenged with flagellin, CXCL10 was expressed in the basal epithelial cells and a group of CXCX3 positive cells were seen lining as a single layer underneath the epithelial layer in the stroma; these cells were shown to be natural killer (NK) cells [32]. NK cells have been shown to possess pro-angiogenic property in non-small cell lung cancer [48], to remodel maternal vasculature in

early pregnancy [49], and to induce angio-genesis by promoting enhanced VEGF expression by macrophages in the cornea micropocket assays and the laser-induced choroidal neovascularization mouse models (C57BL/6) [50]. It is, however, unclear if the pro-angiogenic effects are related to inflammation mediated by NK cells which are known to be a major source of interferon-γ [50]. Since our data indicates that epithelial expression of CXCL10 is anti-angiogenic, it is likely that CXCL10, in addition to being a chemokine, may directly act on both hem-and lymph-endothelial cells. Our data showed that corneal epithelial-expressed CXCL10 prevents both hem- and lymph-angiogenesis, but may not prevent the entrance of CD31- and Lyve1-positive cells into inflamed corneas.

Our study for the first-time links the effects of CXCL10 on corneal angiogenesis to the expression of MMP-13, while TIMP1 appears not to be involved in the process. In addition, MMP13 was shown to play a role in angiogenesis in cancer and during wound healing [51, 52]. While the levels of CXCL10 had an inverse relationship with that of MMP13, targeting MMP13 had no effects on the epithelium-expressionion of CXCL10 in sutured corneas, suggesting that MMP13 expression is downstream of CXCL10. MMP13 is a highly inducible gene and insulin-like growth factors, TGF-β1, IL-1β and TNFα have been shown to induce its expression in different tissues [53]. MMP-13 is thought to be the major enzyme responsible for cartilage collagen degradation, which is driven by IL-1 cytokine. The IL-1 signaling, however, suppressed by interferon-γ, resulting in downregulation of MMP-13 [54, 55]. Our previous study revealed that basal epithelium expressed CXCL10 recruits NK cells to line underneath the basement membrane of the epithelium and infection results in the influx of NK cells that express IFN-γ which in turn induces the persistent expression of CXCL10 during infection. Hence, CXCL10 as an early response and highly inducible gene that not only initiate but also maintain the expression of IFN-γ, resulting in the suppression of IL-1-induced expression of MMP13. One of the underlying mechanisms for MMP13 to promote angiogenesis is to breakdown heparin sulfate proteoglycan and release the entrapped bFGF, a potent angiogenic growth factor [56] and/or cleave CTGF, which blocks angiogenic activity of VEGF by complex formation [51]. MMP13 has been linked to osteoarthritic cartilage [57, 58], rheumatoid syn-ovium [59, 60], chronic cutaneous ulcers [61, 62], intestinal ulcerations [63, 64], and chronic periodontitis [65, 66]. We have shown that *P. aeruginosa* infection induced the expression of MMP13 in the epithelium and utilized it to degrade the underlying basement membrane, resulting in the invasion of the pathogens into the stroma. Topical co-application of MMP13i with gatifloxacin greatly improved the outcomes of *P. aeruginosa* keratitis, including accelerated opacity dissolution; decreased inflammation, cellular infiltration, and collagen disorganization; and basement membrane preservation. Thus, as a downstream effector of CXCL10, MMP13 can be targeted using MMP13-specific inhibitors, designed to treat osteoarthritis and rheumatoid arthritis without the side effects often associated with many non-selective MMP inhibitors [67, 68], for treating pathogenic neovascularization in the cornea and other tissues [69].

Finally, we showed that CXCL10 eye drops can protect the corneas from *C. albicans*-induced hem- and lymph-angiogenesis as well as preserve the structural integrity of the corneal sub-basal sensory nerve plexus. Thus, CXCL10, via derived peptide [70], or AAV-CXCL10 vector can be topically applied to the ocular surface to reduce or prevent corneal

angiogenesis associated with chemical injury and graft rejection, the latter of which is related to corneal lymphangiogenesis [7, 71].

Supplementary Material

Refer to Web version on PubMed Central for supplementary material.

References

1. Ellenberg D, Azar DT, Hallak JA, et al. Novel aspects of corneal angiogenic and lymphangiogenic privilege. Prog Retin Eye Res. 2010; 29:208–248. [PubMed: 20100589]
2. Singh N, Tiem M, Watkins R, et al. Soluble vascular endothelial growth factor receptor 3 is essential for corneal alymphaticity. Blood. 2013; 121:4242–4249. [PubMed: 23476047]
3. Zhang H, Grimaldo S, Yuen D, et al. Combined blockade of VEGFR-3 and VLA-1 markedly promotes high-risk corneal transplant survival. Invest Ophthalmol Vis Sci. 2011; 52:6529–6535. [PubMed: 21715348]
4. Yuen D, Pytowski B, Chen L. Combined blockade of VEGFR-2 and VEGFR-3 inhibits inflammatory lymphangiogenesis in early and middle stages. Invest Ophthalmol Vis Sci. 2011; 52:2593–2597. [PubMed: 21273538]
5. Han KY, Azar DT, Sabri A, et al. Characterization of the interaction between endostatin short peptide and VEGF receptor 3. Protein Pept Lett. 2012; 19:969–974. [PubMed: 22512651]
6. Regenfuss B, Bock F, Cursiefen C. Corneal angiogenesis and lymphangiogenesis. Curr Opin Allergy Clin Immunol. 2012; 12:548–554. [PubMed: 22951910]
7. Patel SP, Dana R. Corneal lymphangiogenesis: implications in immunity. Semin Ophthalmol. 2009; 24:135–138. [PubMed: 19437348]
8. Montezuma SR, Vavvas D, Miller JW. Review of the ocular angiogenesis animal models. Semin Ophthalmol. 2009; 24:52–61. [PubMed: 19373687]
9. Gimenez F, Suryawanshi A, Rouse BT. Pathogenesis of herpes stromal keratitis—a focus on corneal neovascularization. Prog Retin Eye Res. 2013; 33:1–9. [PubMed: 22892644]
10. Ellenberg D, Azar DT, Hallak JA, et al. Novel aspects of corneal angiogenic and lymphangiogenic privilege. Prog Retin Eye Res. 2010; 29:208–248. [PubMed: 20100589]
11. Chang JH, Gabison EE, Kato T, et al. Corneal neovascularization. Curr Opin Ophthalmol. 2001; 12:242–249. [PubMed: 11507336]
12. Hajrasouliha AR, Funaki T, Sadrai Z, et al. Vascular endothelial growth factor-C promotes alloimmunity by amplifying antigen-presenting cell maturation and lymphangiogenesis. Invest Ophthalmol Vis Sci. 2012; 53:1244–1250. [PubMed: 22281820]
13. Hos D, Bock F, Dietrich T, et al. Inflammatory corneal (lymph) angiogenesis is blocked by VEGFR-tyrosine kinase inhibitor ZK 261991, resulting in improved graft survival after corneal transplantation. Invest Ophthalmol Vis Sci. 2008; 49:1836–1842. [PubMed: 18436817]
14. Cursiefen C, Chen L, Dana MR, et al. Corneal lymphangiogenesis: evidence, mechanisms, and implications for corneal transplant immunology. Cornea. 2003; 22:273–281. [PubMed: 12658100]
15. Zheng Y, Lin H, Ling S. Clinicopathological correlation analysis of (lymph) angiogenesis and corneal graft rejection. Mol Vis. 2011; 17:1694–1700. [PubMed: 21738399]
16. Cogan D. Corneal vascularization. Invest Ophthalmol Vis Sci. 1962; 1:253–261.
17. Yuan X, Wilhelmus KR. Corneal neovascularization during experimental fungal keratitis. Mol Vis. 2009; 15:1988–1996. [PubMed: 19816603]
18. Sun RL, Jones DB, Wilhelmus KR. Clinical characteristics and outcome of *Candida keratitis*. Am J Ophthalmol. 2007; 143:1043–1045. [PubMed: 17524775]
19. Wu TG, Wilhelmus KR, Mitchell BM. Experimental keratomycosis in a mouse model. Invest Ophthalmol Vis Sci. 2003; 44:210–216. [PubMed: 12506077]
20. He J, Lian C, Fang Y, et al. Effect of CXCL10 receptor antagonist on islet cell apoptosis in a type I diabetes rat model. Int J Clin Exp Pathol. 2015; 8:14542–14548. [PubMed: 26823775]

21. Wang X, Wang Q, Wu J, et al. Increased expression of CXCR3 and its ligands in vitiligo patients and CXCL10 as a potential clinical marker for vitiligo. Br J Dermatol. 2016; 174:1318–1326. [PubMed: 26801009]
22. Maru SV, Holloway KA, Flynn G, et al. Chemokine production and chemokine receptor expression by human glioma cells: role of CXCL10 in tumour cell proliferation. J Neuroimmunol. 2008; 199:35–45. [PubMed: 18538864]
23. Strieter RM, Kunkel SL, Arenberg DA, et al. Interferon gamma-inducible protein 10 (IP-10), a member of the C-X-C chemokine family, is an inhibitor of angiogenesis. Biochem Biophys Res Commun. 1995; 210:51–57. [PubMed: 7537965]
24. Kudo Y, Iizuka S, Yoshida M, et al. Matrix metallopro-teinase-13 (MMP-13) directly and indirectly promotes tumor angiogenesis. J Biol Chem. 2012; 287:38716–38728. [PubMed: 22992737]
25. Cole AM, Ganz T, Liese AM, et al. Cutting edge: IFN-inducible ELR-CXC chemokines display defensin-like antimicrobial activity. J Immunol. 2001; 167:623–627. [PubMed: 11441062]
26. Qin S, Rottman JB, Myers P, et al. The chemokine receptors CXCR3 and CCR5 mark subsets of T cells associated with certain inflammatory reactions. J Clin Invest. 1998; 101:746–754. [PubMed: 9466968]
27. Cao W, Liu YJ. Innate immune functions of plasmacytoid dendritic cells. Curr Opin Immunol. 2007; 19:24–30. [PubMed: 17113765]
28. Mohan K, Cordeiro E, Vaci M, et al. CXCR3 is required for migration to dermal inflammation by normal and in vivo activated T cells: differential requirements by CD4 and CD8 memory subsets. Eur J Immunol. 2005; 35:1702–1711. [PubMed: 15884054]
29. Yuan J, Liu Z, Lim T, et al. CXCL10 inhibits viral replication through recruitment of natural killer cells in coxsackievirus B3-induced myocarditis. Circ Res. 2009; 104:628–638. [PubMed: 19168435]
30. Cole AM, Ganz T, Liese AM, et al. Cutting edge: IFN-inducible ELR-CXC chemokines display defensin-like antimicrobial activity. J Immunol. 2001; 167:623–627. [PubMed: 11441062]
31. Yoon GS, Dong C, Gao N, et al. Interferon regulatory factor-1 in flagellin-induced reprogramming: potential protective role of CXCL10 in cornea innate defense against *Pseudomonas aeruginosa* infection. Invest Ophthalmol Vis Sci. 2013; 54:7510–7521. [PubMed: 24130180]
32. Liu X, Gao N, Dong C, et al. Flagellin-induced expression of CXCL10 mediates direct fungal killing and recruitment of NK cells to the cornea in response to candida albicans infection. Eur J Immunol. 2014; 44:2667–2679. [PubMed: 24965580]
33. Mimura T, Amano S, Usui T, et al. Expression of vascular endothelial growth factor C and vascular endothelial growth factor receptor 3 in corneal lymphangiogenesis. Exp Eye Res. 2001; 72:71–78. [PubMed: 11133184]
34. Cao Y, Linden P, Farnebo J, et al. Vascular endothelial growth factor C induces angiogenesis in vivo. Proc Natl Acad Sci U S A. 1998; 95:14389–14394. [PubMed: 9826710]
35. Wigle JT, Harvey N, Detmar M, et al. An essential role for Prox1 in the induction of the lymphatic endothelial cell phenotype. EMBO J. 2002; 21:1505–1513. [PubMed: 11927535]
36. Wigle JT, Oliver G. Prox1 function is required for the development of the murine lymphatic system. Cell. 1999; 98:769–778. [PubMed: 10499794]
37. Cursiefen C, Maruyama K, Jackson DG, et al. Time course of angiogenesis and lymphangiogenesis after brief corneal inflammation. Cornea. 2006; 25:443–447. [PubMed: 16670483]
38. Gu X, Zhang J, Brann DW, et al. Brain and retinal vascular endothelial cells with extended life span established by ectopic expression of telomerase. Invest Ophthalmol Vis Sci. 2003; 44:3219–3225. [PubMed: 12824274]
39. Hos D, Cursiefen C. Lymphatic vessels in the development of tissue and organ rejection. Adv Anat Embryol Cell Biol. 2014; 214:119–141. [PubMed: 24276891]
40. Freiberg FJ, Matlach J, Grehn F, et al. Postoperative sub-conjunctival bevacizumab injection as an adjunct to 5-fluo-rouracil in the management of scarring after trabeculectomy. Clin Ophthalmol. 2013; 7:1211–1217. [PubMed: 23814458]
41. Petsoglou C, Balaggan KS, Dart JK, et al. Subconjunctival bevacizumab induces regression of corneal neovascularisation: a pilot randomised placebo-controlled double-masked trial. Br J Ophthalmol. 2013; 97:28–32. [PubMed: 23087419]

42. Lai LJ, Xiao X, Wu JH. Inhibition of corneal neovascularization with endostatin delivered by adeno-associated viral (AAV) vector in a mouse corneal injury model. J Biomed Sci. 2007; 14:313–322. [PubMed: 17373573]
43. Cheng HC, Yeh SI, Tsao YP, et al. Subconjunctival injection of recombinant AAV-angiostatin ameliorates alkali burn induced corneal angiogenesis. Mol Vis. 2007; 13:2344–2352. [PubMed: 18199977]
44. Zhou SY, Xie ZL, Xiao O, et al. Inhibition of mouse alkali burn induced-corneal neovascularization by recombinant adenovirus encoding human vasohibin-1. Mol Vis. 2010; 16:1389–1398. [PubMed: 20680097]
45. Hellstrom M, Harvey AR. Retinal ganglion cell gene therapy and visual system repair. Curr Gene Ther. 2011; 11:116–131. [PubMed: 21291357]
46. Shen FH, Wang SW, Yeh TM, et al. Absence of CXCL10 aggravates herpes stromal keratitis with reduced primary neutrophil influx in mice. J Virol. 2013; 87:8502–8510. [PubMed: 23720717]
47. Wuest TR, Carr DJ. Dysregulation of CXCR3 signaling due to CXCL10 deficiency impairs the antiviral response to herpes simplex virus 1 infection. J Immunol. 2008; 181:7985–7993. [PubMed: 19017990]
48. Bruno A, Focaccetti C, Pagani A, et al. The proangiogenic phenotype of natural killer cells in patients with non-small cell lung cancer. Neoplasia. 2013; 15:133–142. [PubMed: 23441128]
49. Rajagopalan S, Long EO. Cellular senescence induced by CD158d reprograms natural killer cells to promote vascular remodeling. Proc Natl Acad Sci U S A. 2012; 109:20596–20601. [PubMed: 23184984]
50. Lee H, Schlereth SL, Park EY, et al. A novel pro-angiogenic function for interferon-gamma-secreting natural killer cells. Invest Ophthalmol Vis Sci. 2014; 55:2885–2892. [PubMed: 24713481]
51. Hattori N, Mochizuki S, Kishi K, et al. MMP-13 plays a role in keratinocyte migration, angiogenesis, and contraction in mouse skin wound healing. Am J Pathol. 2009; 175:533–546. [PubMed: 19590036]
52. Kudo Y, Iizuka S, Yoshida M, et al. Matrix metallopro-teinase-13 (MMP-13) directly and indirectly promotes tumor angiogenesis. J Biol Chem. 2012; 287:38716–38728. [PubMed: 22992737]
53. Leeman MF, Curran S, Murray GI. The structure, regulation, and function of human matrix metalloproteinase-13. Crit Rev Biochem Mol Biol. 2002; 37:149–166. [PubMed: 12139441]
54. Ahmad R, Qureshi HY, El Mabrouk M, et al. Inhibition of interleukin 1-induced matrix metalloproteinase 13 expression in human chondrocytes by interferon gamma. Ann Rheum Dis. 2007; 66:782–789. [PubMed: 17179173]
55. Ahmad R, El Mabrouk M, Sylvester J, et al. Human osteoarthritic chondrocytes are impaired in matrix metallopro-teinase-13 inhibition by IFN-gamma due to reduced IFN-gamma receptor levels. Osteoarthritis Cartilage. 2009; 17:1049–1055. [PubMed: 19285161]
56. Whitelock JM, Murdoch AD, Iozzo RV, et al. The degradation of human endothelial cell-derived perlecan and release of bound basic fibroblast growth factor by stromelysin, collagenase, plasmin, and heparanases. J Biol Chem. 1996; 271:10079–10086. [PubMed: 8626565]
57. Wang X, Manner PA, Horner A, et al. Regulation of MMP-13 expression by RUNX2 and FGF2 in osteoarthritic cartilage. Osteoarthritis Cartilage. 2004; 12:963–973. [PubMed: 15564063]
58. Stahle-Backdahl M, Sandstedt B, Bruce K, et al. Collage-nase-3 (MMP-13) is expressed during human fetal ossification and re-expressed in postnatal bone remodeling and in rheumatoid arthritis. Lab Invest. 1997; 76:717–728. [PubMed: 9166290]
59. Moore BA, Aznavoorian S, Engler JA, et al. Induction of collagenase-3 (MMP-13) in rheumatoid arthritis synovial fibroblasts. Biochim Biophys Acta. 2000; 1502:307–318. [PubMed: 11040455]
60. Wernicke D, Seyfert C, Gromnica-Ihle E, et al. The expression of collagenase 3 (MMP-13) mRNA in the synovial tissue is associated with histopathologic type II synovitis in rheumatoid arthritis. Autoimmunity. 2006; 39:307–313. [PubMed: 16891219]
61. Toriseva MJ, Ala-aho R, Karvinen J, et al. Collagenase-3 (MMP-13) enhances remodeling of three-dimensional collagen and promotes survival of human skin fibroblasts. J Invest Dermatol. 2007; 127:49–59. [PubMed: 16917496]

62. Vaalamo M, Mattila L, Johansson N, et al. Distinct populations of stromal cells express collagenase-3 (MMP-13) and collagenase-1 (MMP-1) in chronic ulcers but not in normally healing wounds. J Invest Dermatol. 1997; 109:96–101. [PubMed: 9204962]

63. Rath T, Roderfeld M, Halwe JM, et al. Cellular sources of MMP-7, MMP-13 and MMP-28 in ulcerative colitis. Scand J Gastroenterol. 2010; 45:1186–1196. [PubMed: 20568971]

64. Vaalamo M, Karjalainen-Lindsberg ML, Puolakkainen P, et al. Distinct expression profiles of stromelysin-2 (MMP-10), collagenase-3 (MMP-13), macrophage metalloelastase (MMP-12), and tissue inhibitor of metalloproteinases-3 (TIMP-3) in intestinal ulcerations. Am J Pathol. 1998; 152:1005–1014. [PubMed: 9546361]

65. Hernandez Rios M, Sorsa T, Obregon F, et al. Proteolytic roles of matrix metalloproteinase (MMP)-13 during progression of chronic periodontitis: initial evidence for MMP-13/MMP-9 activation cascade. J Clin Periodontol. 2009; 36:1011–1017. [PubMed: 19929954]

66. Hernandez M, Martinez B, Tejerina JM, et al. MMP-13 and TIMP-1 determinations in progressive chronic periodontitis. J Clin Periodontol. 2007; 34:729–735. [PubMed: 17716308]

67. Kalva S, Saranyah K, Suganya PR, et al. Potent inhibitors precise to S1’ loop of MMP-13, a crucial target for osteoarthritis. J Mol Graph Model. 2013; 44:297–310. [PubMed: 23938376]

68. Jungel A, Ospelt C, Lesch M, et al. Effect of the oral application of a highly selective MMP-13 inhibitor in three different animal models of rheumatoid arthritis. Ann Rheum Dis. 2010; 69:898–902. [PubMed: 19497915]

69. Vandenbroucke RE, Dejonckheere E, Libert C. A therapeutic role for matrix metalloproteinase inhibitors in lung diseases? Eur Respir J. 2011; 38:1200–1214. [PubMed: 21659416]

70. Yates-Binder CC, Rodgers M, Jaynes J, et al. An IP-10 (CXCL10)-derived peptide inhibits angiogenesis. PLoS ONE. 2012; 7:e40812. [PubMed: 22815829]

71. Hos D, Schlereth SL, Bock F, et al. Antilymphangiogenic therapy to promote transplant survival and to reduce cancer metastasis: what can we learn from the eye? Semin Cell Dev Biol. 2015; 38:117–130. [PubMed: 25460541]

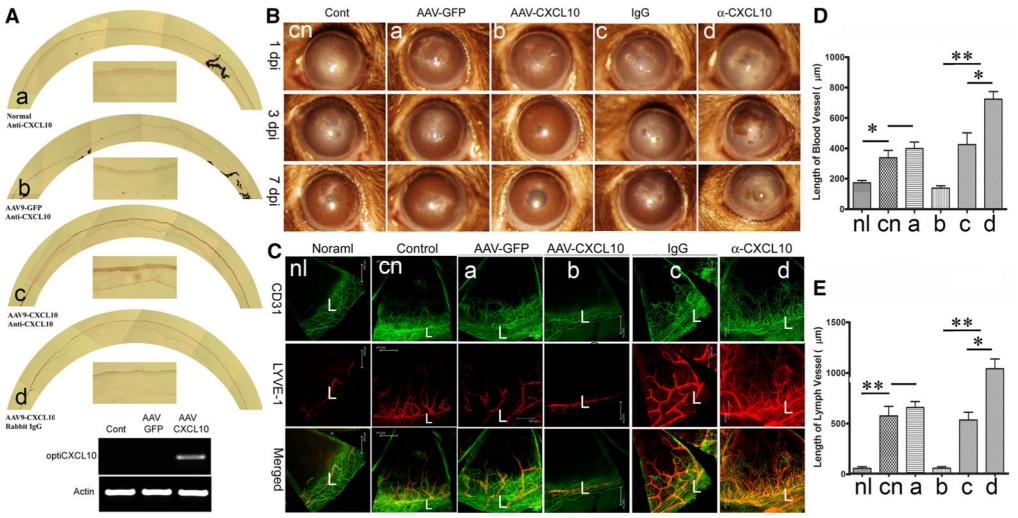

Fig. 1.

Epithelial levels of CXCL10 control *C. albicans* induced angiogenesis in the cornea. **A.** AAV-9 mediated epithelial expression of CXCL10 in the cornea. AAV9-GFP or AAV9CXCL10 were injected subconjunctivally and at day 14 corneas were collected and the expression of CXCL10 was assessed using immunohistochemistry and RT-PCR. **B.** To assess the role of exogenously expressed or endogenously induced CXCL10, AAV9-GFP or AAV9CXCL10, CXCL10 neutralizing antibody, or nonspecific IgG as the control, was injected subconjunctuvally. The treated corners, 14 days post AAV9 infection or 6 h post antibody injection, were inoculated with *C. albicans* and photographed at the indicated days p.i. with slid lamp. **C.** The blood and lymph vessels were visualized by whole mount staining of the corneas with CD31 for blood and LYVE1 for lymph vessels. L: Limbus. To quantify neovascularization in infected corneas, the lengths of blood **(D)** or lymph vessels **(E)** from the edge of the limbal region to the tip of vessels was measured by Image J. The results are representative of two independent experiments ($N = 3$ each) and indicated p values were generated using unpaired Student's t test. $^{**}p < 0.01$, $^{*}p < 0.05$

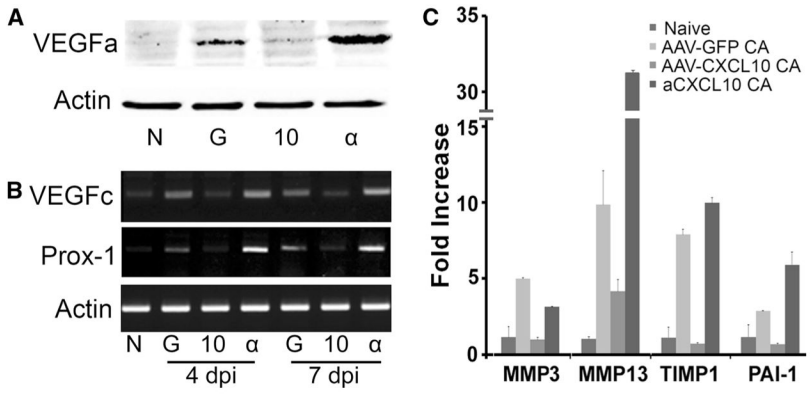

Fig. 2.

CXCL10 inhibition of hem-and lymph-angiogenesis was CXCR3 dependent. GFP or CXCL10 transfected corneas were treated with anti-CXCR3 antibody by subconjunctival injection before *C. albicans* inoculation. **A.** Slid lamp images showed *C. albicans* keratitis and vessels at 7 days infection. **B.** The blood and lymph vessels were visualized by whole mount staining of the corneas with CD31 for blood (*green*) and LYVE1 for lymph (*red*) vessels. L: limbus. The lengths of blood **(C)** and lymph vessels were measured by Image J **(D)**. The results are representative of two independent experiments ($N = 3$ each) and indicated p values were generated using unpaired Student's t test. $^{**}p < 0.01$, $^{*}p < 0.05$. (Color figure online)

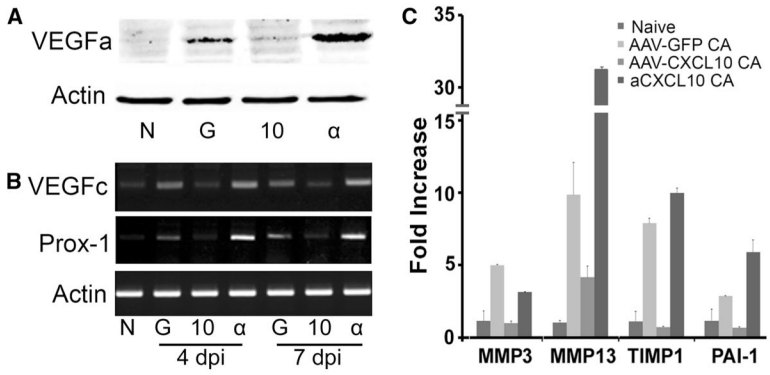

Fig. 3.

Expression of angiogenesis-related genes in *C. albicans* infected corneas expressing or neutralized CXCL10. **A.** Mouse corneas were subconjunctivally injected AAV9-CXCL10, AAV9-GFP for transfection or anti-CXCL10 and inoculated with *C. albicans.* Western blotting probed 4 dpi corneal extracts for VEGFa with actin as the internal control. **B.** RT PCR to detecting the expression of VEGFc and lymph vessel marker Prox-1 using RNA extracted from 4 to 7 dpi corneas. **C.** Realtime PCR validation of proteome array data for MMP2, MMP13, TIMP1, Serpine1, as well as MMP13 which was on the list of Proteome Profiler for angiogenic factors (sF3). The results are representative of two independent experiments ($N = 3$ each) and indicated p values were generated using unpaired Student's t test. $^{**}p < 0.01$, $^{*}p < 0.05$

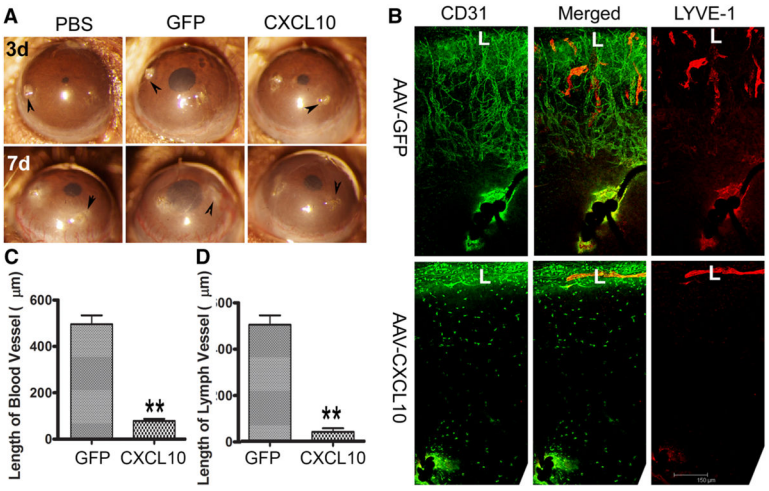

Fig. 4.

CXCL10 blocks suture-induced angiogenesis in the cornea. B6 mouse corneas were infected with AAV9-GFP or AAV9CXCL10. At day 14 post AAV9 infection, three non-penetrating sutures were placed. **A.** At 3 (3d) and 7 (7d) days post suture, corneas were photographed. *Arrowheads*, suture sites. **B.** At 7 days post suture, the corneas were excised, and subjected to whole mount staining with CD31 for blood (*green*) and LYVE1 for lymph (*red*) vessels, respectively. L: limbus. **C.** Quantitation of the lengths of blood vessels from the edge of the limbal region to the tips of vessels in the infected corneas. **D.** Quantitation of the lengths of lymph vessels from the edge of the limbal region to the tips of vessels in the corneas. The results are representative of two independent experiments ($N = 3$ each) and indicated p values were generated using unpaired Student's t test. $^{**}p < 0.01$, $^{*}p < 0.05$. (Color figure online)

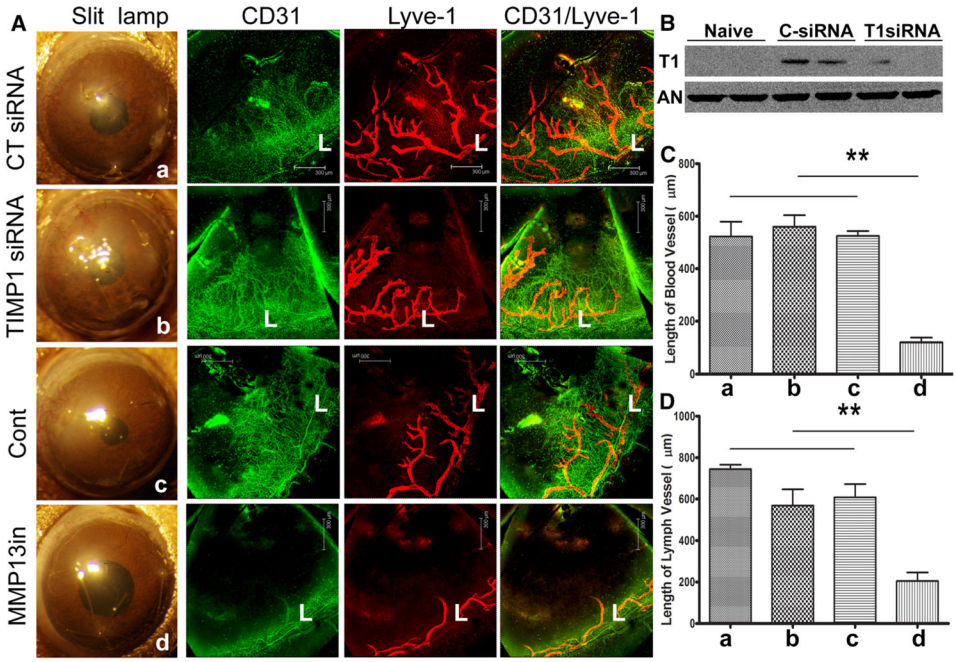

Fig. 5.

Effects of MMP13 and TIMP1 on angiogenesis in the sutured mouse corneas. **A.** B6 mouse corneas were subconjunctivally injected CT siRNA or TIMP1 siRNA twice 24 and 4 h or MMP13 inhibitor 4 h prior to suture. Three non-penetrating sutures were placed to the treated corneas. At 7 days post suture, the corneas were photographed, excised, and subjected to whole mount staining with CD31 for blood (*green*) and LYVE1 for lymph (*red*) vessels, respectively. L: limbus. **B.** Quantitation of blood vessels from the edge of the limbal region to the tips of vessels in the infected corneas. **C.** Quantitation of lymph vessels from the edge of the limbal region to the tip of vessels in the infected corneas. The results are representative of two independent experiments ($N = 3$ each) and indicated p values were generated using unpaired Student's t test. $^{**}p < 0.01$, $^{*}p < 0.05$. (Color figure online)

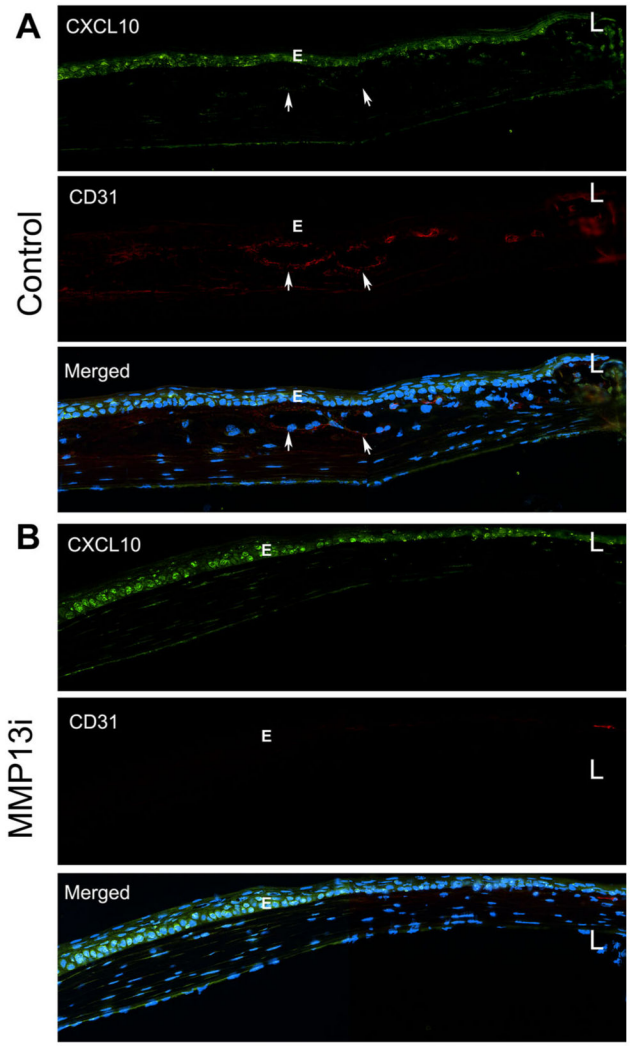

Fig. 6.

MMP13 inhibitor upregulats the expression of CXCL10 and blocks angiogenesis in sutured corneas. C57BL/6 mouse corneas ($n = 3$ for each condition) were subconjunctivally with injected control solution or MMP13 inhibitor for 4 h, followed by sutured as described in Fig. 5, then stained with CXCL10 and CD31. **A.** Vehicle injected corneas with visible vessels in the stroma marked with *arrows*. **B.** MMP13i injected corneas with no detectable vessels or DC31 positive cells. E: epithelium, L: limbus

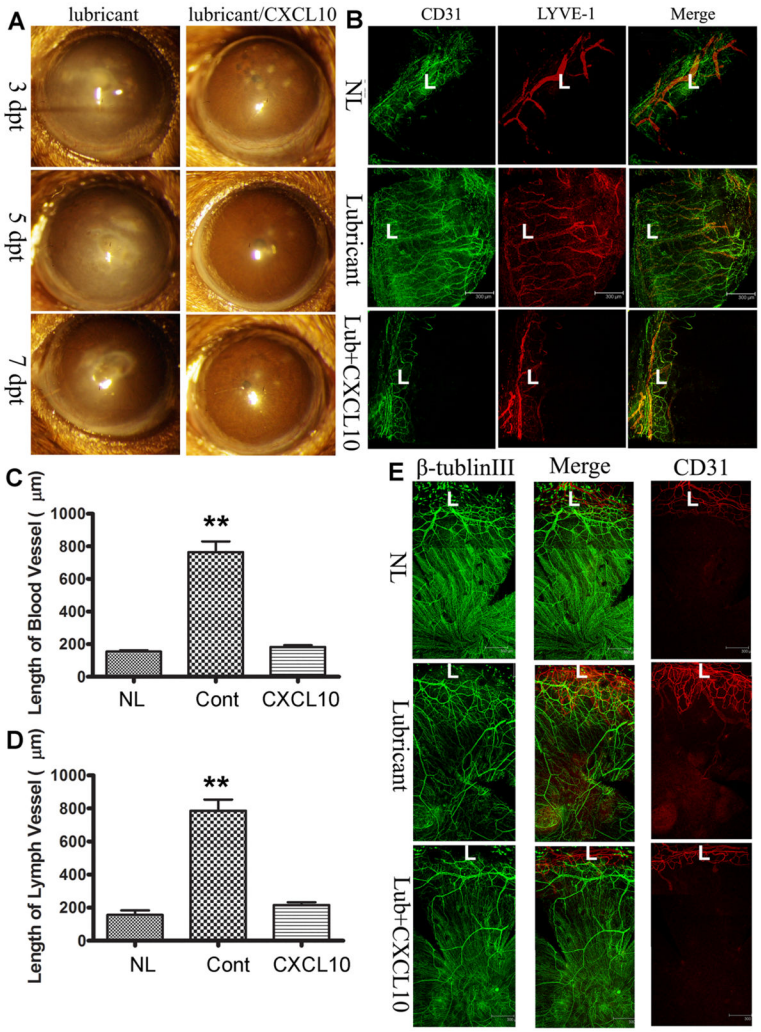

Fig. 7.

Topical CXCL10 prevents neovascularization and preserve the subbasal nerve plexus. **A.** Human recombinant CXCL10 (25 μg/ml) was dissolved in Soothe eye lubricant. *C. albicans* infected corneas were treated topically with or without CXCL10 starting 16 hpi, 3 times daily and the eyes were photographed at 3, 5, and 7 days post CXCL10 treatment. **B.** Whole mount detection of blood (CD31, *green*) and lymphatic (LYVE-1, *red*) vessels of *C. albicans* infected corneas at 7 dpi. L: limbus. **C.** Quantitation of the lengths of blood vessels from the edge of the limbal region to the tips of vessels in the infected corneas. **E.** Quantitation of the lengths of lymph vessels from the edge of the limbal region to the tips of vessels in the infected corneas. The control was the naïve corneas without any treatment (NL). The results are representative of two independent experiments ($N = 3$ each) and indicated p values were generated using unpaired Student's t test. $^{**}p < 0.01$, $^{*}p < 0.05$. **E.** Whole mount detection of blood (CD31, *red*) vessels and sensory nerves (tubulin III, *green*) in *C. albicans* infected corneas treated topically with or without CXCL10 starting 6 hpi, naïve corneas (NL) as the control. L: limbus. (Color figure online)